No.92 **Feb. 2022**

ISSN 0917-2211

Variable Star Bulletin

Analysis of the IW And star ASAS J071404+7004.3

Taichi Kato,[1] Kiyoshi Kasai,[2] Elena P. Pavlenko,[3,4] Nikolaj V. Pit,[3] Aleksei A. Sosnovskij,[3] Hiroshi Itoh,[5] Hidehiko Akazawa,[6] Stephen M. Brincat,[7] Leonid E. Keir,[8] Sergei N. Udovichenko,[8] Yusuke Tampo,[1] Naoto Kojiguchi,[1] Masaaki Shibata,[1] Yasuyuki Wakamatsu,[1] Tamás Tordai,[9] Tonny Vanmunster,[10] Charles Galdies[11]

tkato@kusastro.kyoto-u.ac.jp

[1] Department of Astronomy, Kyoto University, Sakyo-ku, Kyoto 606-8502, Japan
[2] Baselstrasse 133D, CH-4132 Muttenz, Switzerland
[3] Federal State Budget Scientific Institution "Crimean Astrophysical Observatory of RAS", Nauchny, 298409, Republic of Crimea
[4] V. I. Vernadsky Crimean Federal University, 4 Vernadskogo Prospekt, Simferopol, 295007, Republic of Crimea
[5] Variable Star Observers League in Japan (VSOLJ), 1001-105 Nishiterakata, Hachioji, Tokyo 192-0153, Japan
[6] Akazawa Funao Observartory, 107 Funao, Funaocho, Kurashiki, Okayama 710-0261, Japan
[7] Flarestar Observatory, San Gwann SGN 3160, Malta
[8] Astronomical Observatory of Odessa I. I. Mechnikov National University, Marazlievskaya 1v, 65014 Odessa, Ukraine
[9] Polaris Observatory, Hungarian Astronomical Association, Laborc utca 2/c, 1037 Budapest, Hungary
[10] Center for Backyard Astrophysics Belgium, Walhostraat 1A, B-3401 Landen, Belgium
[11] Institute of Earth Systems, University of Malta, Msida, MSD 2080, Malta

Received 2022 Feb. 23

Abstract

We made a time-resolved photometric campaign of the bright cataclysmic variable ASAS J071404+7004.3 in 2020. Inight et al. (2022, arXiv/2109.14514) recently published time-resolved optical spectroscopy, X-ray observations and long- and short-term optical variations. Although their results were correct in many parts, they classified ASAS J071404+7004.3 as a VY Scl-type novalike object. By comparing the ASAS-SN data of this object and the IW And-type object HO Pup, we showed that their type classification was incorrect. ASAS J071404+7004.3 showed outbursts from a standstill followed by shallow dips, which is the defining characteristic of an IW And star. This object predominantly showed states with low-amplitude dwarf nova-type oscillations, some of which could be identified as the "heartbeat"-type state as a variety of the IW And-type phenomenon. The low state described by Inight et al. (2022) was not a true low state of a VY Scl star, but a dwarf nova-type state with increased outburst amplitudes. Both ground-based (our campaign) and TESS observations detected orbital variations whose periods [0.136589(5) d by the ground-based campaign and 0.1366476(3) d by the TESS data] are in very good agreement with the one obtained by radial-velocity studies by Inight et al. (2022). The standstill in 2019–2020 in ASAS J071404+7004.3 was not brighter than its dwarf nova-type states. The brightest moment of this object occurred when the amplitudes of dwarf nova-type variations were large, which challenges the widely accepted interpretation that standstills in Z Cam stars occur when the mass-transfer rates are high.

1 Introduction

Inight et al. (2022) reported on the recently identified nearby, bright ($V \sim 12$) cataclysmic variable (CV) ASAS J071404+7004.3. This object was identified as the optical counterpart of the X-ray source 1RXS J071404.0+700413 by Kiraga and Stępień (2013) by examining light variations of ROSAT All Sky Survey sources (Voges et al. 1999) using the northern twin (ASAS-N) of the All-Sky Automated Survey (ASAS: Pojmański 2002). This object was unique among the objects identified by Kiraga and Stępień (2013) in that it was classified as a miscellaneous variable star with a period of 22.44 d.

Inight et al. (2022) published time-resolved optical spectroscopy, X-ray observations and long- and short-term optical variations. The object was confirmed to be a CV with an orbital period of 0.1366454(1) d. Inight et al. (2022) compared the long-term light curve of this object with the AAVSO light curves of prototypical objects of CV subtypes: Z Cam (Z Cam star), V513 Cas (IW And star) and VY Scl (VY Scl star) and concluded that the object belongs to the VY Scl-type CVs based on the visual similarity of the light curve rather than detailed comparisons.

This object was introduced to us by a baavss-alert message "Request for help in monitoring ASAS J071404+7004.3" requested by Boris Gänsicke and posted by Jeremy Shears on 2020 February 7[1]. Upon this message, one of the authors (TK) examined All-Sky Automated Survey for Supernovae (ASAS-SN) Sky Patrol data (Shappee et al. 2014; Kochanek et al. 2017) and readily identified it as an IW And star (T. Kato, vsnet-alert 23944[2] on 2020 February 7) based on the heartbeat-type variation with shallow dips in 2017 and the presence of standstills. This identification was quickly reflected on the AAVSO Variable Star Index (VSX: Watson et al. 2006)[3]. It is strange that there was no trace of examination of this type identification in Inight et al. (2022) and we clarify the reasons of the apparent discrepancy in the type classification.

In the following section, we describe the results from ASAS-SN observations. We conducted our own campaign of time-resolved photometry by the VSNET Collaboration (Kato et al. 2004), which was aimed to detect possible negative superhumps (T. Kato, vsnet-alert 23949[4]) motivated by the presence of negative superhumps (a tilted disk) in the IW And star KIC 9406652 (Gies et al. 2013; Kimura et al. 2020a; Kimura and Osaki 2021) and a possible suggestion that a tilted disk might be responsible for the IW And-type phenomenon (Kimura et al. 2020a). The log of observations is shown in table 1. The R and I bands refer to Kron-Cousins systems. We also analyzed Transiting Exoplanet Survey Satellite (TESS) observations.[5] The full light-curve is available at the Mikulski Archive for Space Telescope (MAST[6]).

Table 1: Log of observations of ASAS J071404+7004.3.

Start*	End*	mag†	error‡	N§	obs‖	band#
58887.2403	58887.4579	11.562	0.003	246	Van	R
58887.2413	58887.4583	12.020	0.003	246	Van	V
58888.4555	58888.5833	11.594	0.003	168	Van	R
58888.4561	58888.5827	12.056	0.003	164	Van	V
58889.6340	58889.7702	11.841	0.003	156	Van	V

*JD−2400000.
†Mean magnitude.
‡1σ of the mean magnitude.
§Number of observations.
‖Observer's code: Aka (H. Akazawa), BSM (S. Brincat), CRI (Crimean Astrophys. Obs.), GCH (C. Galdies), Ioh (H. Itoh), KU1 (Kyoto U. rooftop obs.), Kai (K. Kasai), May (Mayaki Obs.), Trt (T. Tordai), Van (T. Vanmunster).
#Filter. "C" means unfiltered.

[1] Although baavss-alert mailing list on yahoo had a publicly accessible archive, this service has already been discontinued and the message is not currently publicly available.
[2] <http://ooruri.kusastro.kyoto-u.ac.jp/mailarchive/vsnet-alert/23944>.
[3] <https://www.aavso.org/vsx/index.php?view=detail.top&oid=300502>.
[4] <http://ooruri.kusastro.kyoto-u.ac.jp/mailarchive/vsnet-alert/23949>.
[5] <https://tess.mit.edu/observations/>.
[6] <http://archive.stsci.edu/>.

Table 1: Log of observations of ASAS J071404+7004.3 (continued).

Start*	End*	mag†	error‡	N§	obs‖	band#
58890.0932	58890.2128	11.816	0.002	359	Ioh	C
58890.2151	58890.3351	-0.286	0.003	163	CRI	C
58890.2334	58890.4270	11.844	0.005	100	BSM	V
58890.2344	58890.4280	11.640	0.006	89	BSM	I
58890.4491	58890.5404	12.175	0.007	9	Van	B
58890.4504	58890.5417	11.865	0.012	9	Van	V
58892.2501	58892.5173	11.620	0.014	19	Van	R
58892.5180	58892.5190	12.152	0.001	5	Van	V
58893.0409	58893.2323	-0.431	0.001	1358	KU1	C
58893.4654	58893.5545	-0.273	0.004	104	CRI	C
58893.5152	58893.5499	12.135	0.009	6	Van	B
58893.5166	58893.5512	11.841	0.017	6	Van	V
58893.5676	58893.6573	12.060	0.002	330	May	R
58894.1140	58894.1698	-0.409	0.002	432	KU1	C
58894.3092	58894.3092	12.093	–	1	Van	CV
58894.3103	58894.5522	11.889	0.014	9	Van	V
58894.5149	58894.5509	12.146	0.010	6	Van	B
58895.2431	58895.4151	11.871	0.006	86	BSM	V
58895.2440	58895.4160	11.690	0.007	79	BSM	I
58895.2490	58895.3544	11.832	0.005	60	GCH	V
58895.2499	58895.3552	11.616	0.006	60	GCH	I
58895.3092	58895.5497	12.195	0.015	9	Van	B
58895.3106	58895.5511	11.908	0.014	6	Van	V
58896.2537	58896.4161	11.851	0.005	85	BSM	V
58896.2546	58896.4151	11.634	0.006	57	BSM	I
58896.3134	58896.6055	12.136	0.015	7	Van	B
58896.3150	58896.6069	11.849	0.009	7	Van	V
58896.4278	58896.6302	11.854	0.007	66	GCH	V
58896.4286	58896.6293	11.629	0.005	66	GCH	I
58897.3853	58897.4572	-0.288	0.002	98	CRI	C
58897.4273	58897.4846	11.838	0.006	35	GCH	V
58897.4282	58897.6063	11.639	0.007	62	GCH	I
58898.2358	58898.6443	-0.238	0.001	2003	CRI	C
58898.4455	58898.5999	12.109	0.020	6	Van	B
58898.4469	58898.6014	11.845	0.017	6	Van	V
58899.4977	58899.7251	12.182	0.014	7	Van	B
58899.4990	58899.7239	11.907	0.008	9	Van	V
58900.2339	58900.4157	11.910	0.004	165	BSM	V
58900.4976	58900.7262	12.237	0.009	8	Van	B
58900.4993	58900.7247	11.950	0.005	8	Van	V
58900.5435	58900.6226	11.910	0.005	48	GCH	V
58900.5444	58900.6216	11.689	0.005	47	GCH	I
58901.2503	58901.6714	11.927	0.002	539	Kai	V

*JD−2400000.
†Mean magnitude.
‡1σ of the mean magnitude.
§Number of observations.
‖Observer's code: Aka (H. Akazawa), BSM (S. Brincat), CRI (Crimean Astrophys. Obs.), GCH (C. Galdies), Ioh (H. Itoh), KU1 (Kyoto U. rooftop obs.), Kai (K. Kasai), May (Mayaki Obs.), Trt (T. Tordai), Van (T. Vanmunster).
#Filter. "C" means unfiltered.

Table 1: Log of observations of ASAS J071404+7004.3 (continued).

Start*	End*	mag†	error‡	N§	obs‖	band#
58901.3029	58901.5823	11.874	0.002	318	BSM	V
58901.4978	58901.7253	12.107	0.007	7	Van	B
58901.4988	58901.6578	11.872	0.017	5	Van	V
58901.5416	58901.6152	11.915	0.007	30	GCH	V
58901.5447	58901.6132	11.685	0.004	29	GCH	I
58902.4975	58902.7253	12.183	0.010	9	Van	B
58902.4989	58902.7241	11.909	0.009	9	Van	V
58903.4981	58903.7256	12.176	0.028	7	Van	B
58903.4990	58903.6580	11.829	0.040	6	Van	V
58904.2401	58904.5961	11.931	0.002	407	Kai	V
58904.4981	58904.7253	12.187	0.029	4	Van	B
58904.4989	58904.4994	11.916	0.013	3	Van	V
58905.2309	58905.4930	-2.011	0.002	436	May	R
58905.2415	58905.3582	11.831	0.003	161	Trt	V
58905.3755	58905.5422	-0.251	0.003	226	CRI	C
58906.1052	58906.3658	11.834	0.002	361	Aka	V
58906.2829	58906.4246	-0.247	0.002	192	CRI	C
58906.4837	58906.7254	12.082	0.003	4	Van	B
58906.4853	58906.7242	11.827	0.026	3	Van	V
58906.9395	58907.3708	11.814	0.003	292	Aka	V
58907.4842	58907.6261	12.119	0.009	5	Van	B
58907.4855	58907.7099	11.876	0.015	9	Van	V
58908.3710	58908.5595	11.832	0.002	450	Trt	CV
58910.5706	58910.5711	11.628	0.006	3	Van	R
58910.9375	58911.3143	11.800	0.003	270	Aka	V
58911.3220	58911.5347	-0.276	0.002	288	CRI	C
58911.4681	58911.4686	11.643	0.007	3	Van	R
58911.9661	58912.0521	11.799	0.004	55	Aka	V
58913.3184	58913.6768	11.791	0.001	871	Trt	V
58913.9270	58914.0178	11.776	0.006	73	Aka	V
58914.0531	58914.2712	11.766	0.002	456	Ioh	V
58914.2568	58914.4465	11.793	0.004	209	BSM	V
58914.9345	58915.0146	11.815	0.003	167	Ioh	V
58916.2513	58916.4514	11.926	0.003	253	Kai	V
58916.9406	58917.0958	11.924	0.003	147	Aka	V
58918.9692	58919.1906	11.842	0.002	359	Ioh	V
58919.9386	58920.0664	11.833	0.004	119	Aka	V
58920.2469	58920.4573	11.865	0.002	243	BSM	V
58920.2670	58920.5717	11.878	0.002	401	Kai	V
58920.9181	58921.0824	11.881	0.003	151	Aka	V
58921.2463	58921.5264	-0.249	0.002	379	CRI	C
58921.2469	58921.4200	11.823	0.005	200	BSM	V
58921.3510	58921.3514	11.580	0.007	3	Van	R

*JD−2400000.
†Mean magnitude.
‡1σ of the mean magnitude.
§Number of observations.
‖Observer's code: Aka (H. Akazawa), BSM (S. Brincat), CRI (Crimean Astrophys. Obs.), GCH (C. Galdies), Ioh (H. Itoh), KU1 (Kyoto U. rooftop obs.), Kai (K. Kasai), May (Mayaki Obs.), Trt (T. Tordai), Van (T. Vanmunster).
#Filter. "C" means unfiltered.

Table 1: Log of observations of ASAS J071404+7004.3 (continued).

Start*	End*	mag†	error‡	N§	obs‖	band#
58921.9225	58922.0375	11.836	0.012	12	Aka	V
58922.2563	58922.4496	11.929	0.002	229	Kai	V
58922.9169	58923.0817	11.905	0.004	141	Aka	V
58923.2440	58923.3678	11.919	0.003	124	BSM	V
58923.2583	58923.3547	11.664	0.007	42	GCH	I
58923.2913	58923.6167	11.944	0.003	318	Kai	V
58924.2966	58924.6162	11.939	0.002	438	Kai	V
58925.9374	58926.0609	11.835	0.004	118	Aka	V
58926.2837	58926.6095	11.904	0.003	306	Kai	V
58926.9214	58927.0259	11.822	0.004	100	Aka	V
58927.9136	58928.0794	11.862	0.004	158	Aka	V
58928.2683	58928.5974	11.908	0.002	405	Kai	V
58928.9217	58929.0517	11.855	0.003	124	Aka	V
58929.9151	58930.0732	11.820	0.003	150	Aka	V
58931.2772	58931.5853	11.876	0.002	379	Kai	V
58931.9134	58932.0502	11.806	0.005	130	Aka	V
58932.2744	58932.5878	11.867	0.002	430	Kai	V
58932.9478	58933.0523	11.815	0.004	100	Aka	V
58933.2719	58933.5594	11.882	0.002	370	Kai	V
58933.9427	58934.0441	11.838	0.005	97	Aka	V
58934.2866	58934.5844	11.890	0.003	399	Kai	V
58935.2794	58935.5188	11.902	0.002	330	Kai	V
58939.2897	58939.5744	11.906	0.003	346	Kai	V
58940.2760	58940.5717	11.885	0.002	322	Kai	V
58941.2824	58941.5637	11.907	0.003	253	Kai	V
58942.2825	58942.5454	11.927	0.003	332	Kai	V
58943.2586	58943.4255	12.081	0.002	326	May	R
58945.2525	58945.4978	11.939	0.002	440	May	R
58945.2642	58945.4158	11.800	0.002	190	BSM	V
58945.2677	58945.3942	11.585	0.003	82	GCH	I
58945.2915	58945.5449	11.830	0.002	302	Kai	V
58946.2911	58946.5505	11.833	0.002	340	Kai	V
58946.9222	58947.2099	11.827	0.002	610	Ioh	V
58947.2909	58947.5459	11.878	0.002	335	Kai	V
58947.9265	58948.2262	11.884	0.002	649	Ioh	V
58948.2619	58948.4155	11.931	0.003	185	BSM	V
58948.2682	58948.4491	11.698	0.003	134	GCH	I
58948.2861	58948.5414	11.963	0.002	335	Kai	V
58949.2820	58949.4997	12.034	0.002	428	May	R
58949.2993	58949.4091	11.624	0.005	56	GCH	I
58950.0043	58950.1393	11.758	0.002	340	Ioh	V
58953.9519	58954.2054	11.876	0.002	695	Ioh	V

*JD−2400000.
†Mean magnitude.
‡1σ of the mean magnitude.
§Number of observations.
‖Observer's code: Aka (H. Akazawa), BSM (S. Brincat), CRI (Crimean Astrophys. Obs.), GCH (C. Galdies), Ioh (H. Itoh), KU1 (Kyoto U. rooftop obs.), Kai (K. Kasai), May (Mayaki Obs.), Trt (T. Tordai), Van (T. Vanmunster).
#Filter. "C" means unfiltered.

2 Results and discussions

2.1 Long-term light curve

Although the ASAS-SN light curves were shown in Inight et al. (2022), they were either too small (their figure 12) or the important feature was not shown (their figure 2), we provide the full ASAS-SN light curve (figures 1, 2 and 3) together with TESS observations and the VSNET campaign data to show important features.

The most obvious feature is the long-lasting standstill between BJD 2458720 and 2459000 (figure 3, the second panel). It was rather a pity that the start of this standstill was not recorded. This standstill was terminated by an outburst which occurred during TESS observations.

The other parts after BJD 2456950 were dominated by low-amplitude dwarf nova-type variations (starting from the fourth panel of figure 1, most of figure 2 except the final part and figure 3 except the second panel and after BJD 2459550). The 22.44 d period in Kiraga and Stępień (2013) apparently referred to these low-amplitude dwarf nova-type variations. Although such low-amplitude dwarf nova-type variations are also seen in IX Vel (Kato 2021b), the cycle length in ASAS J071404+7004.3 is longer compared to IX Vel with 13–20 d and the profile is different in that variations in ASAS J071404+7004.3 tend to have slower rise and steeper decline as seen in the third panel of figure 2. This feature was interpreted as "inside out" (outburst) in Inight et al. (2022).

2.2 Problem of type classification in Inight et al. (2022)

The main reason why Inight et al. (2022) reached an inadequate classification was that they only consulted the relatively old literature Hameury and Lasota (2014) when referring to IW And stars. It is queer that Inight et al. (2022) referred to the category IW And stars, which term was not mentioned in Hameury and Lasota (2014), but was later defined by Kato (2019). These authors apparently dismissed this later definition and subsequent progress (e.g. Kimura et al. 2020b; Kato et al. 2020, 2021). In Kato (2019); Kimura et al. (2020b), the IW And stars were defined to have the features: (1) Standstills are terminated by brightening in IW And-type objects, unlike fading in Z Cam stars. (2) There are quasi-periodic cycles consisting of a (quasi-)standstill with damping oscillations — brightening which terminates the standstill — often a deep dip (not always present within the same object) and returning to a (quasi-)standstill. When deep dips are not present, the light curve looks like a periodic pattern with gradual rise with an increasing rate to a maximum followed by rapid fading. This pattern is referred to as "heartbeat-type oscillations". It can be confirmed that this is a variety of IW And-type variation since the same object shows both typical IW And-type cycles with deep dips and these heartbeat-type oscillations. The depths of the dips form a continuum from zero (heartbeat-type oscillations) to a few magnitudes in the typical IW And-type cycles. This feature was described for the two objects in FY Vul and HO Pup in Kimura et al. (2020b), and Inight et al. (2022) probably missed modern knowledge of IW And stars. Considering these features, the light curve of ASAS J071404+7004.3 is very similar to that of HO Pup (figures 4 and 5). Just for information, Lee et al. (2021) correctly described HO Pup as an IW And star. The presence of long standstills (second panel in figure 3 and possibly before BJD 2456930 in figure 1) is also similar to the IW And star BO Cet, which showed a long standstill (this object was therefore initially classified as a novalike) lasting for years (Kato et al. 2021).

The second reason is that Inight et al. (2022) did not describe the characteristics of subclasses of CVs correctly. Inight et al. (2022) described IW And stars as showing continual outbursts (not unlike dwarf novae) during the high state (i.e. during the "standstill"). The most obvious feature of the IW And stars, however, is the presence of outbursts at the end of standstills, not during standstills.

Low states in VY Scl stars were also poorly defined (without a reference) and poorly compared with ASAS J071404+7004.3 in Inight et al. (2022). Typical low states of VY Scl stars lasts months to years and there are usually no strong sign of dwarf-nova outbursts during decline despite that the mass-transfer rates decrease. Examples of the light curves and a schematic representation of the lack of dwarf-nova outbursts can be found in Leach et al. (1999). This feature has long been known and the cause of the apparent inconsistency with the disk-instability model has been sought. Leach et al. (1999) suggested heating from a hot white dwarf suppresses thermal instability of the disk. Hameury and Lasota (2002) considered that the magnetism of a white dwarf could truncate the disk, thereby suppressing thermal instability. The presence of magnetism of white dwarfs in VY Scl stars in general, however, has not been apparent by observations. In any case, Inight et al. (2022) did not consider this well-known observational feature of VY Scl stars. The fading episode in ASAS J071404+7004.3

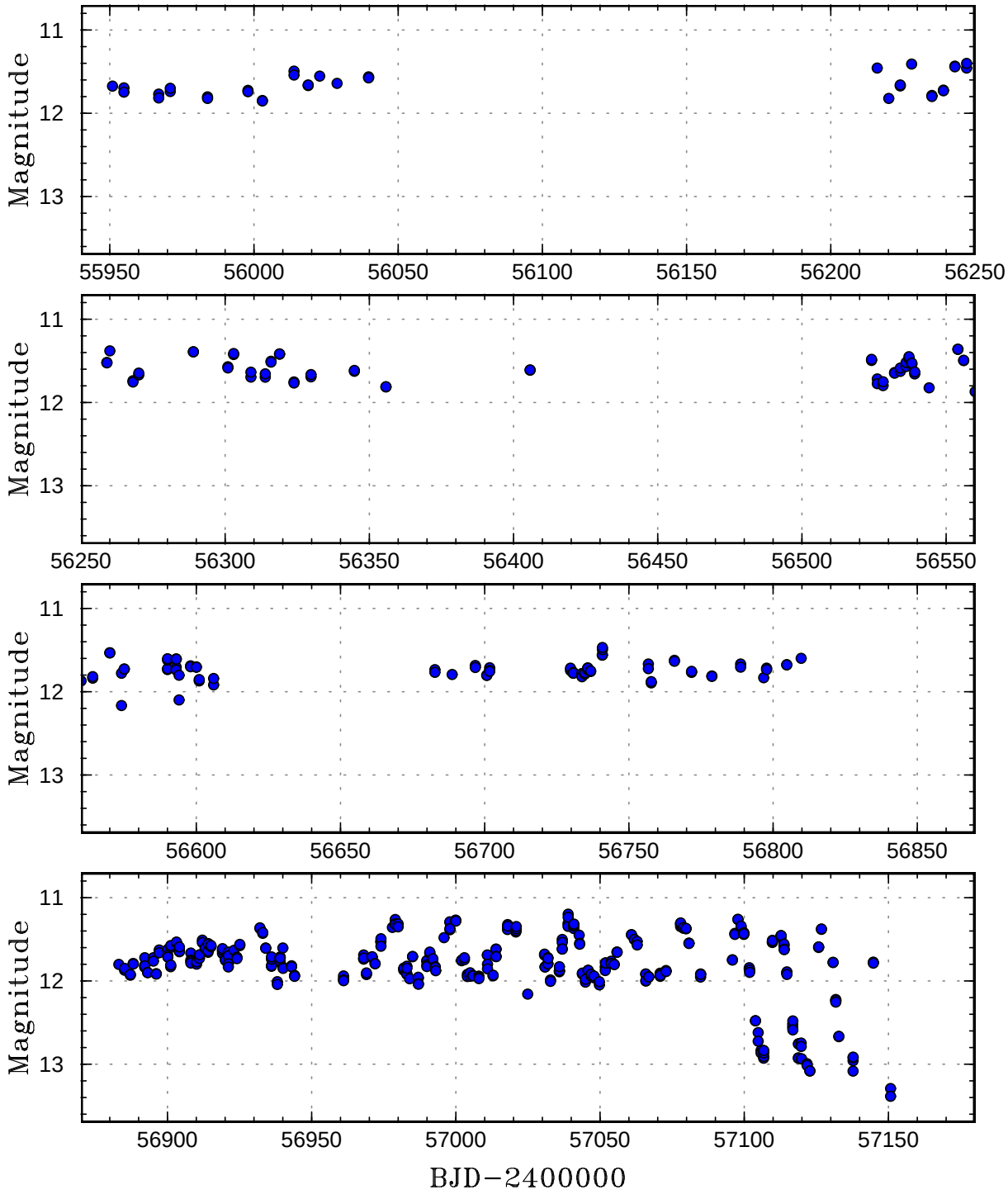

Figure 1: Long-term light curve of ASAS J071404+7004.3 using the ASAS-SN data. All data are in V band. After BJD 2456950, low-amplitude (0.7 mag) dwarf-nova oscillations appeared. After BJD 2457100, the amplitudes of these oscillations became larger (1.6 mag) and the period became shorter.

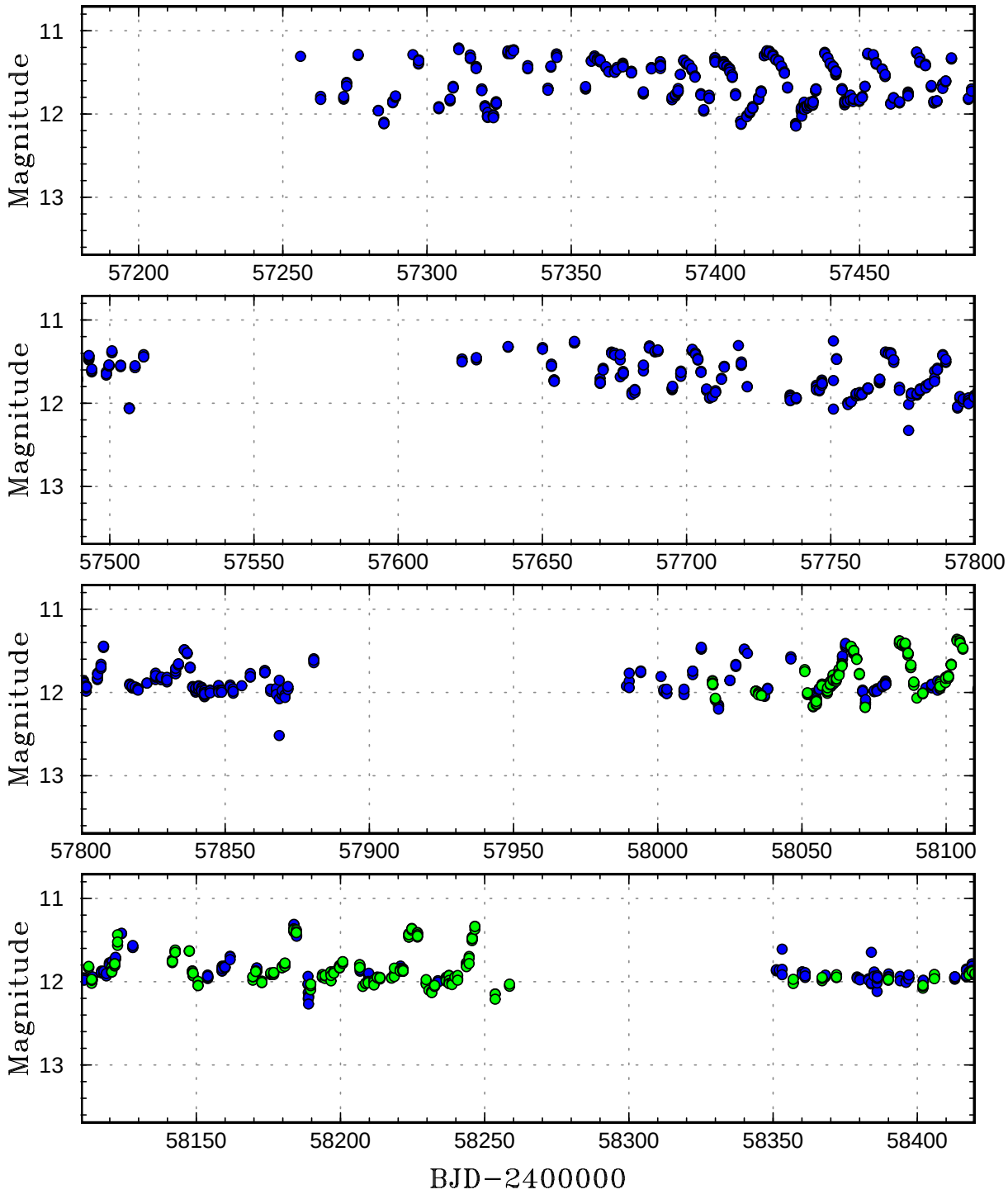

Figure 2: Long-term light curve of ASAS J071404+7004.3 using the ASAS-SN data (2). Blue and green symbols represent V and g observations, respectively. This segment is dominated by low-amplitude dwarf nova-type variations with variable amplitudes and periods. The periods became as short as 10 d. In the latter part of this segment, the periods became longer and the rise to outbursts became slower than the decline. Some outbursts were followed by small dips. This part corresponds to the IW And-type behavior. See figure 5 for a comparison to the IW And star HO Pup.

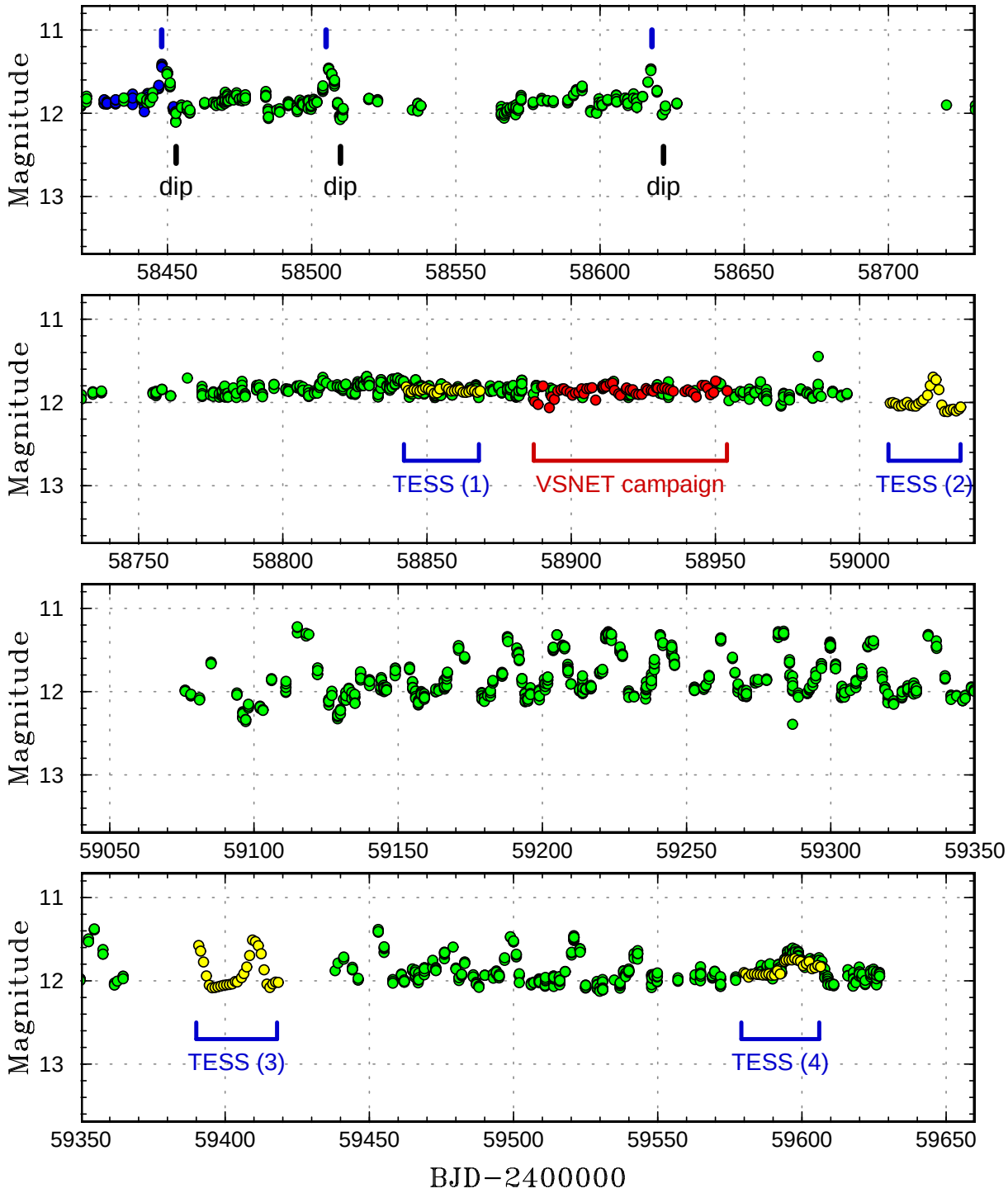

Figure 3: Long-term light curve of ASAS J071404+7004.3 using the ASAS-SN data, TESS data (yellow) and the VSNET campaign data (red). Blue and green symbols for the ASAS-SN data represent V and g observations, respectively. The TESS and VSNET data were binned to 1 d. The initial three runs of of the TESS data were shifted by −0.1 mag to match the ASAS-SN data. The first panel shows the typical behavior of an IW And star. Slowly rising standstills were terminated by outbursts (shown by the upper blue ticks), followed by small dips (shown by the lower ticks). See figure 5 for a comparison to the IW And star HO Pup. The second panel shows the standstill phase. An outburst in the TESS data (2) marked the end of the standstill phase. The third panel is also dominated by dwarf nova-type variations.

was simply a dwarf nova phase with larger amplitudes (as in Z Cam stars) when the mass-transfer rate dropped slightly. It is also apparent from figure 4 that excursions to fainter magnitudes while maintaining dwarf nova-type outbursts happen in other IW And stars. This is probably what happened ASAS J071404+7004.3 after BJD 2457100.

The confusion with the VY Scl-type phenomenon is not, however, surprising. Even the authority of CVs Brian Warner considered dwarf nova-type AM CVn stars, which are currently known as helium counterpart of SU UMa/WZ Sge-type stars in hydrogen-rich CVs (see e.g. Tsugawa and Osaki 1997; Kotko et al. 2012), to be analogous to VY Scl stars at least in the past (Warner 1995).

2.3 Analysis of ground-based time-resolved campaign

We obtained more than 25000 measurements between 2020 February 7 and 2020 April 14. Although some observations are apparently common to the "intensive photometric monitoring of the system using small-aperture telescopes throughout February and March 2020" described in Inight et al. (2022), the majority of the data were obtained by VSOLJ observers, the Crimean Astrophysical Observatory and the Kyoto University team, which are not present in the AAVSO International Database[7] (figures 6 and 7). Inight et al. (2022) did not show any result of period analysis of these ground-based observations. This interval corresponded to the standstill (figure 3, the second panel) and we only searched for periodicities around the orbital period. We used locally-weighted polynomial regression (LOWESS: Cleveland 1979) to remove the long-term trend and applied the Phase Dispersion Minimization (PDM, Stellingwerf 1978) method. The errors of periods by the PDM method were estimated by the methods of Fernie (1989) and Kato et al. (2010). This analysis (figure 8) detected an orbital period of 0.136589(5) d, which agrees with the value by Inight et al. (2022) to better than 0.0005%.

2.4 Period analysis of TESS data

TESS observations have four segments. We performed PDM analysis as in the same way for the ground-based campaign (figures 9, 10, 11 and 12). All segments showed only the orbital signal. We can conclude that that there were neither positive nor negative superhumps regardless of the outbursting phase. This result excludes (at least in this object) a possible suggestion that a tilted disk might be responsible for the IW And-type phenomenon (Kimura et al. 2020a). It has been pointed out that a model involving a tilted disk could not reproduce the variation of the disk radius observed in the IW And star KIC 9406652 (Kimura and Osaki 2021). The absence of negative superhumps has also been reported in other IW And stars (IM Eri: Kato et al. 2020; ST Cha: Kato and Kojiguchi 2021; HO Pup: Lee et al. 2021).

The profile of the orbital variation slightly varied. During the long standstill and one outburst, the profile was almost sinusoidal (figures 9, 10). During another outburst cycle, the maximum of the orbital hump had double peaks (figure 11). During the most recent standstill with some variability, the orbital profile became asymmetric (figure 12). There were no apparent changes in the PDM θ diagrams and these changes were not a result of positive/negative superhumps. Orbital profiles from the TESS observations are shown in figure 13. It appears that the phases of maxima and minima varied slightly. These changes may reflect the changes in the state of the accretion disk or the accretion geometry, and need to be studied in detail.

There were no "embedded precursors" as observed in ST Cha (Kato and Hambsch 2021). There was no enhancement of the orbital signal nor appearance of a long period as observed in a long outburst of the SS Cyg star V363 Lyr (Kato 2021a).

We summarize the values of orbital periods in table 2. We obtained the photometric orbital period from the combined TESS data to be 0.1366476(3) d, which is in very good agreement with the one obtained by the radial-velocity study by Inight et al. (2022).

2.5 Are standstills brighter than dwarf nova-type states?

In figure 14, we show the trend of mean magnitudes (averaged in flux) as we did for IX Vel (Kato 2021b) and ST Cha (Kato and Kojiguchi 2021). The result shows that the 2019–2020 standstill was not brighter than the dwarf nova-type states (IW And-type states) before and after this. This indicates that either standstill or IW And state does not occur as the result of changing mass-transfer rates. This conclusion is the same as in Inight et al. (2022). It would be interesting to note that dwarf nova-type state with relatively large amplitudes in 2015–2016

[7] <https://www.aavso.org>.

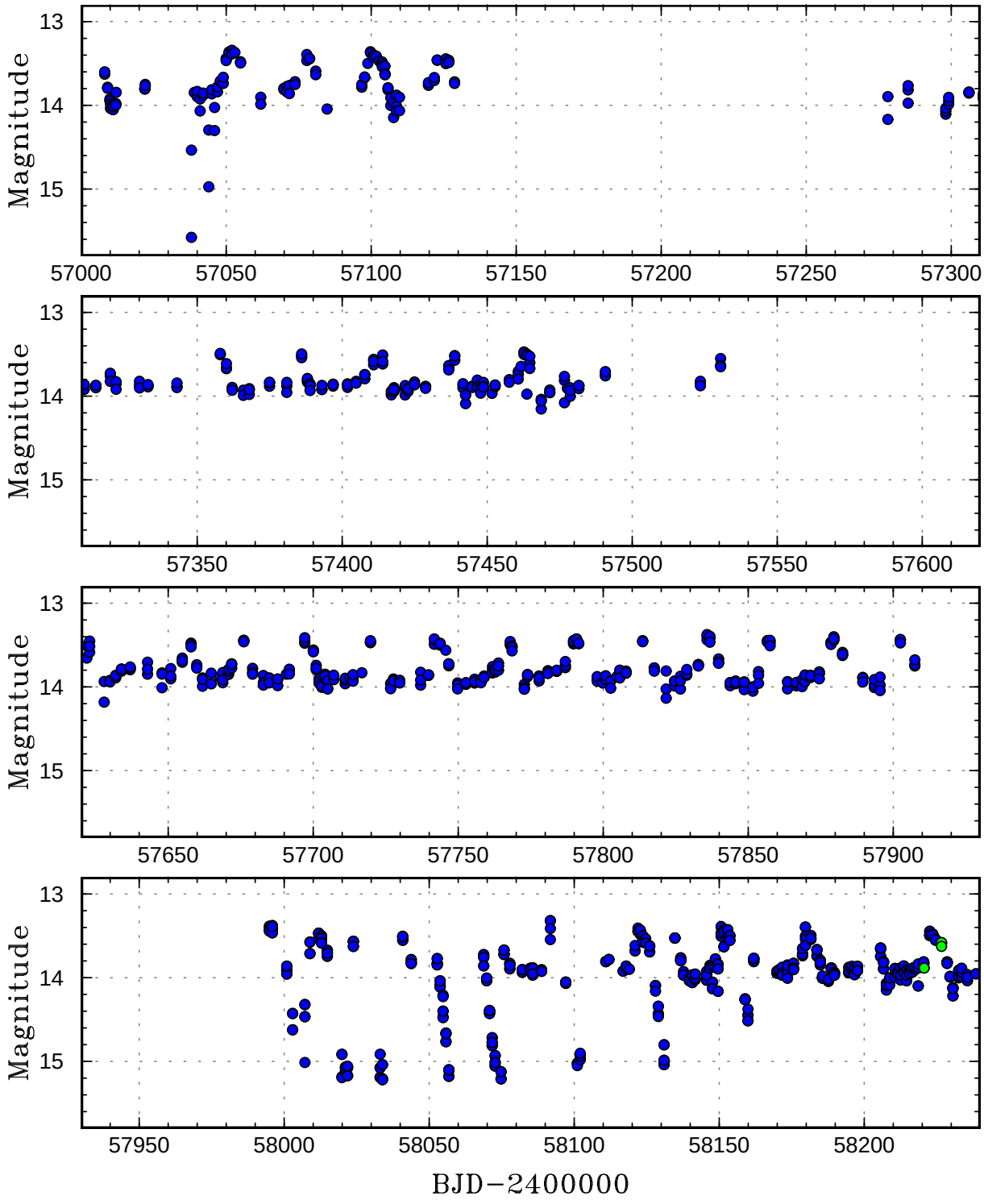

Figure 4: Long-term light curve of HO Pup using the ASAS-SN data. Blue and green symbols represent V and g observations, respectively. The third panel corresponds to "heartbeat-type" oscillations in IW And stars, accompanied by slower rise and steeper decline. This type of variation is considered to be IW And-type cycles simply lacking post-outburst dips. After BJD 2458080, typical IW And-type behavior is seen: standstills terminated by outbursts, followed by dips. It is also apparent that the depths of the dips vary and the dips became inapparent after BJD 2458180, indicating that heartbeat-type oscillations and the typical IW And-type behavior form a smooth continuum.

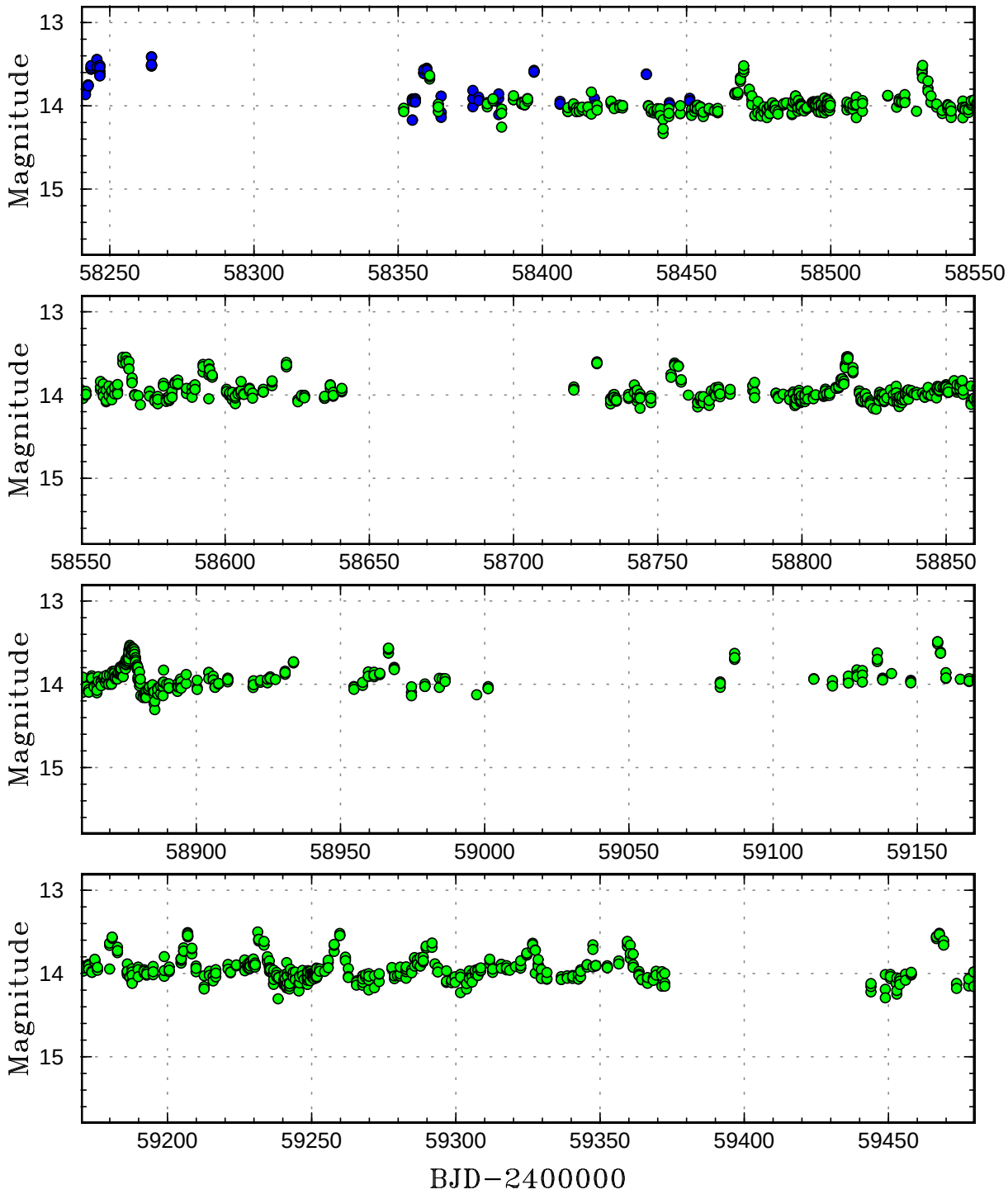

Figure 5: Long-term light curve of HO Pup using the ASAS-SN data (2). Blue and green symbols represent V and g observations, respectively. Most of the time, this star showed heartbeat-type oscillations with variable intervals. This segment is very similar to ASAS J071404+7004.3 between BJD 2458150 and 2458630 (figures 2 and 3).

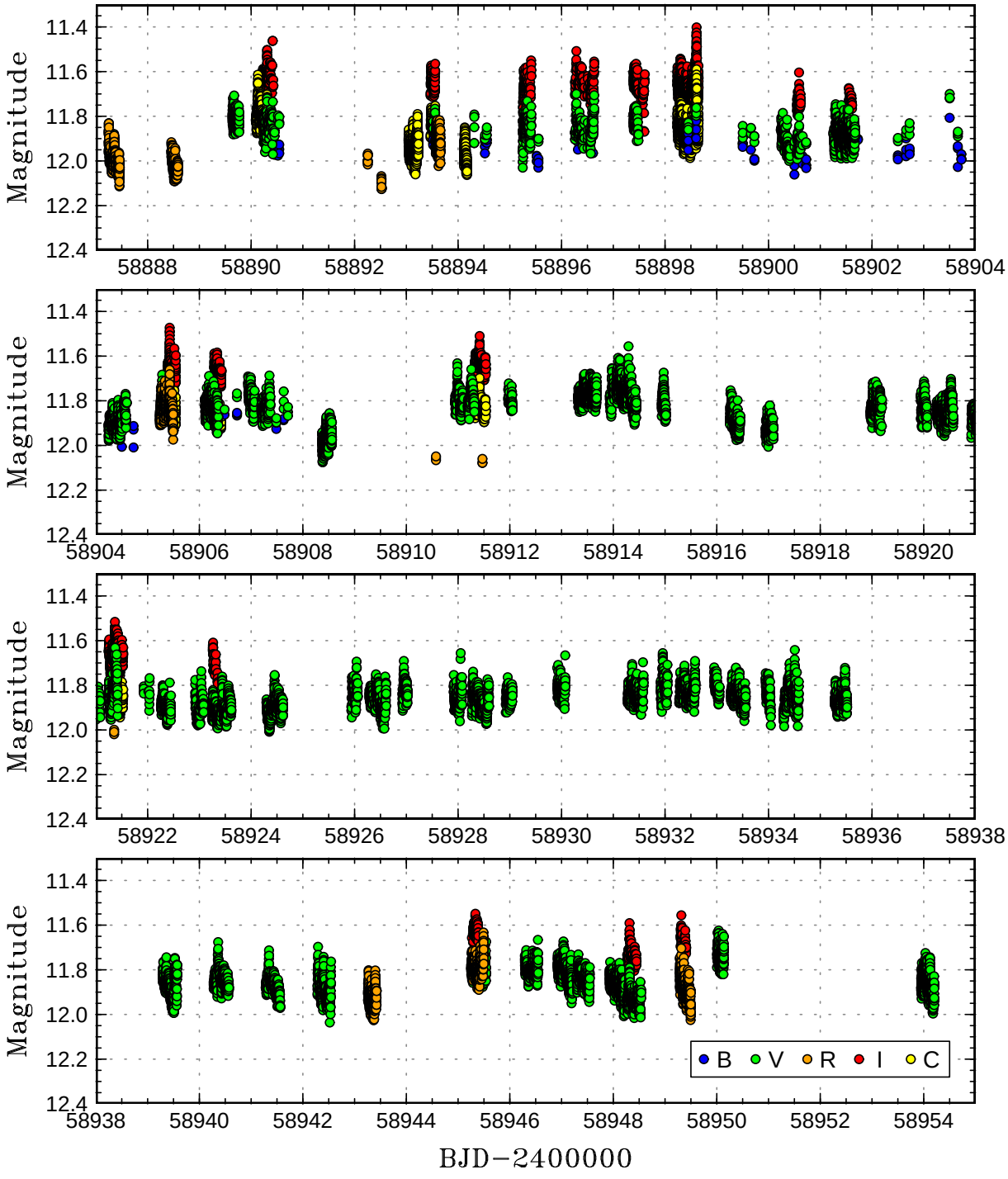

Figure 6: Light curve of ASAS J071404+7004.3 using the ground-based observations obtained by our campaign. The zero points were adjusted by correcting the differences between observers and bands. The color indices against V were determined only for B and I by simultaneous observations, and they are reflected on this figure. The colors corresponded to $B-V$=+0.08 and $V-I$=+0.19. We assumed that the mean magnitudes were the same for V, R and C since there were no simultaneous data for these bands and since the color indices between these bands are expected to be close to zero in this unreddened and disk-dominated CV.

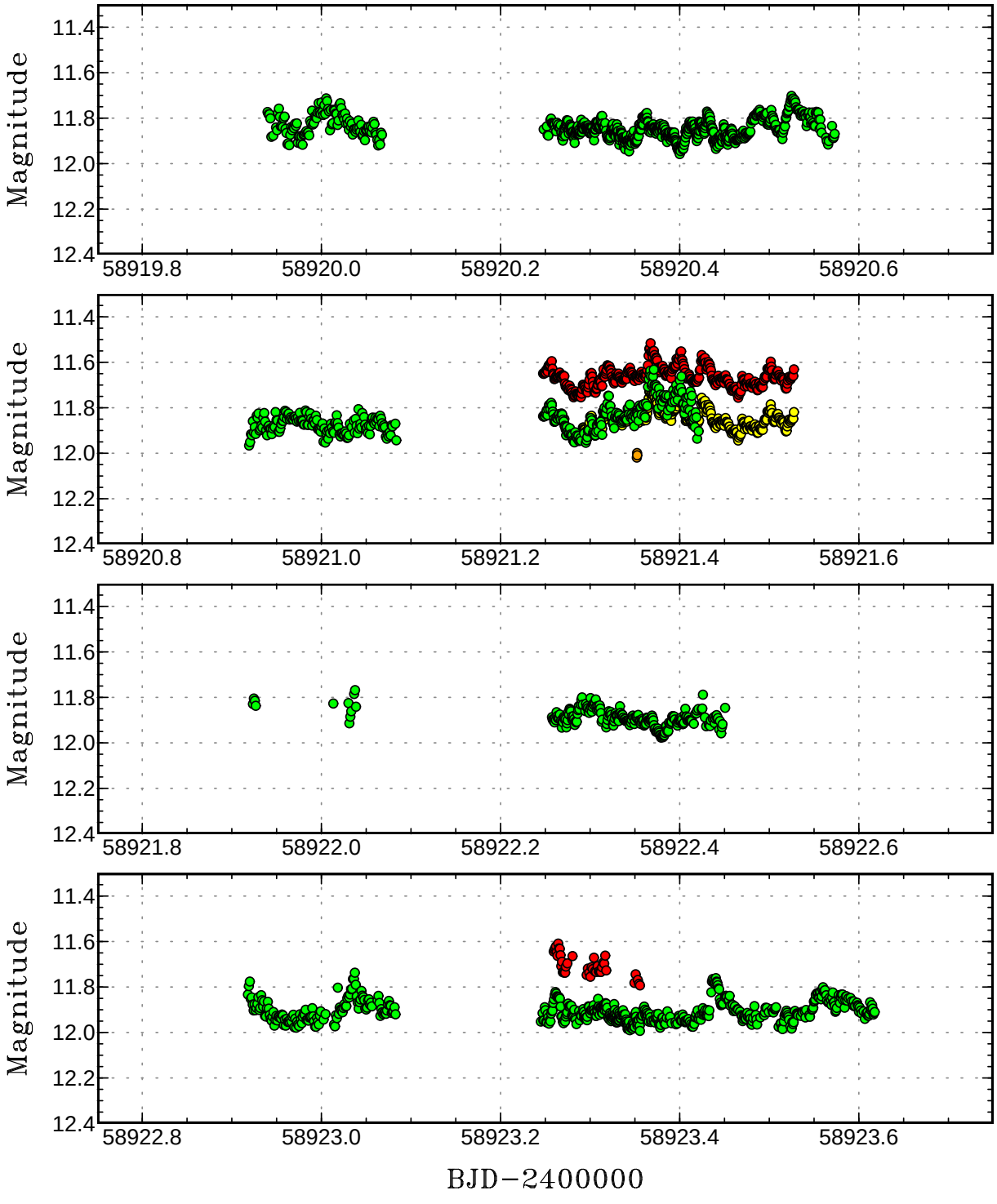

Figure 7: Example of enlarged light curve of ASAS J071404+7004.3 using the ground-based observations obtained by our campaign. The symbols are the same as figure 6.

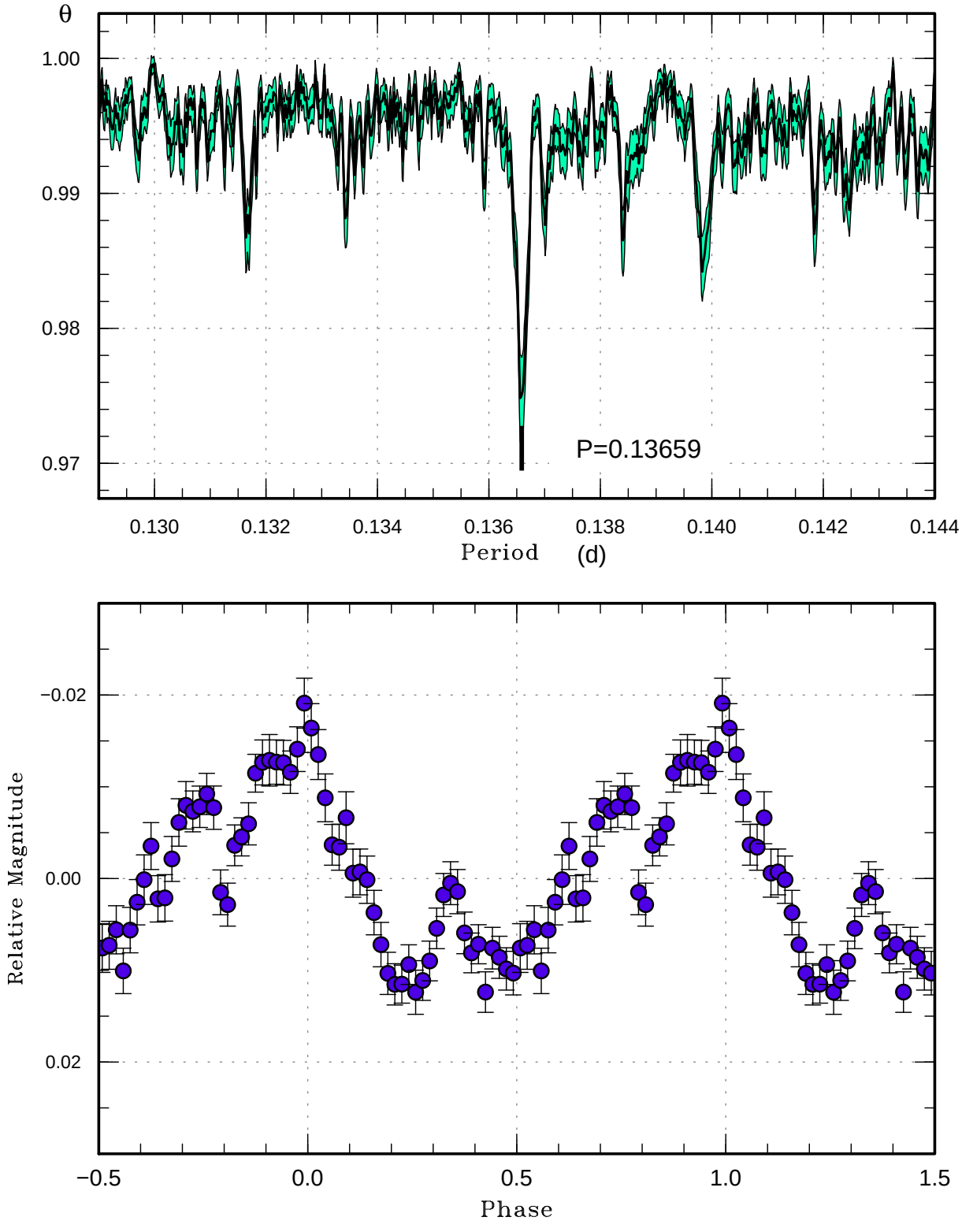

Figure 8: Period analysis of our campaign in 2020 February–April. (Upper): We analyzed 100 samples which randomly contain 50% of observations, and performed the PDM analysis for these samples. The bootstrap result is shown as a form of 90% confidence intervals in the resultant PDM θ statistics. (Lower): Orbital variation.

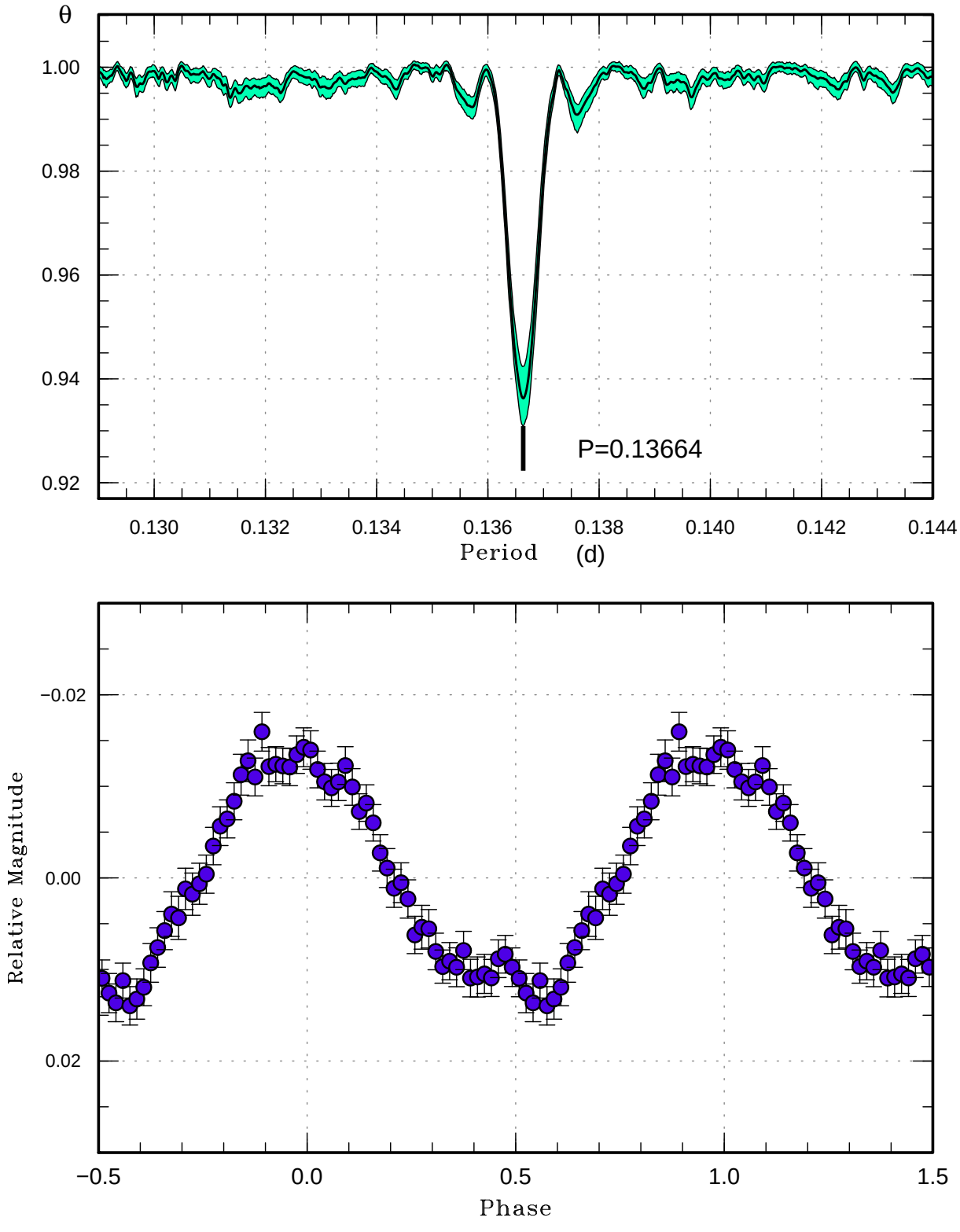

Figure 9: Period analysis of TESS data between BJD 2458842 (2019 December 25) and 2458868 (2020 January 20). These observations correspond to the long standstill phase. (Upper): PDM analysis. (Lower): Orbital variation.

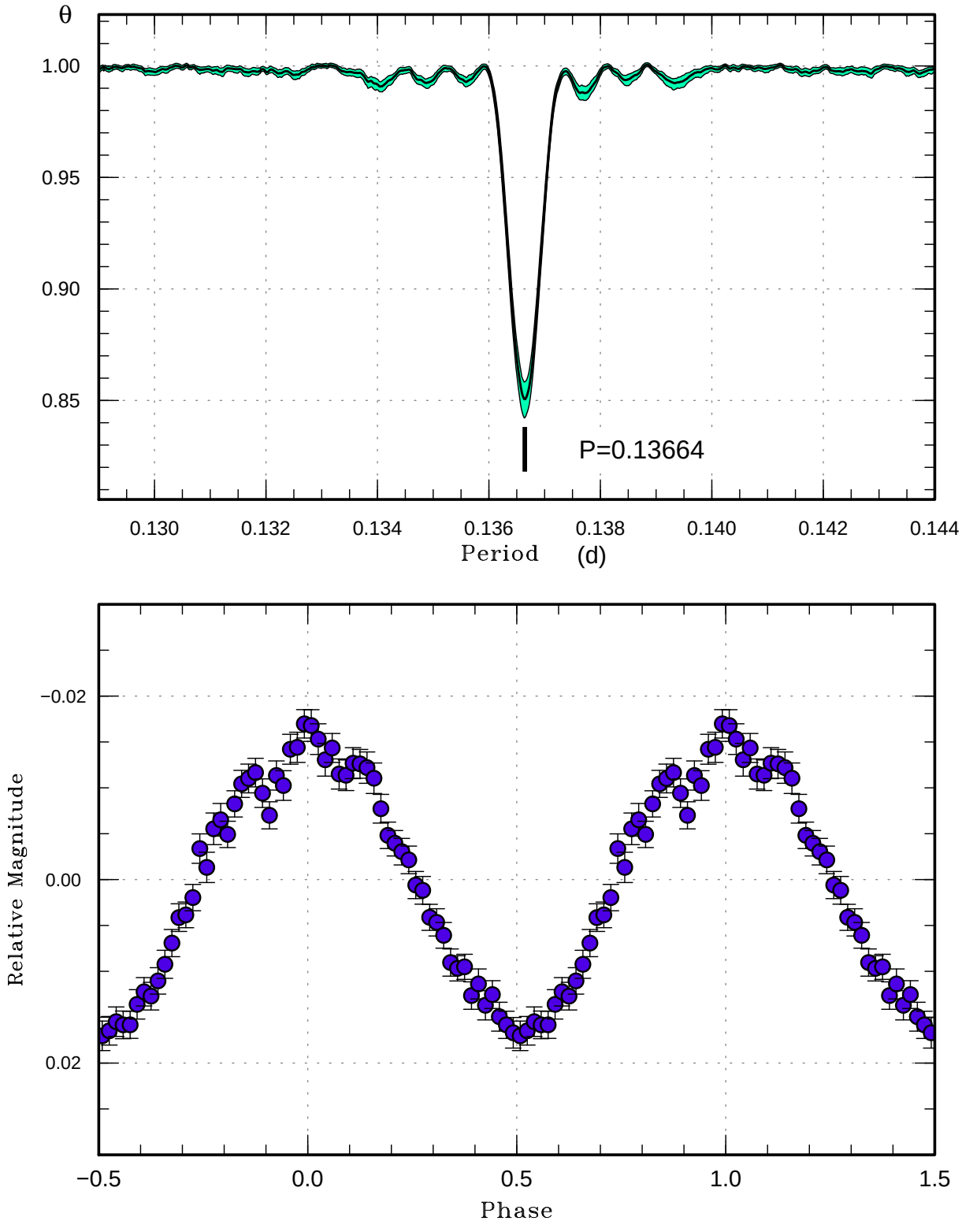

Figure 10: Period analysis of TESS data between BJD 2459010 (2020 June 9) and 2459035 (2020 July 4). These observations covered the outburst that terminated the long standstill phase. (Upper): PDM analysis. (Lower): Orbital variation.

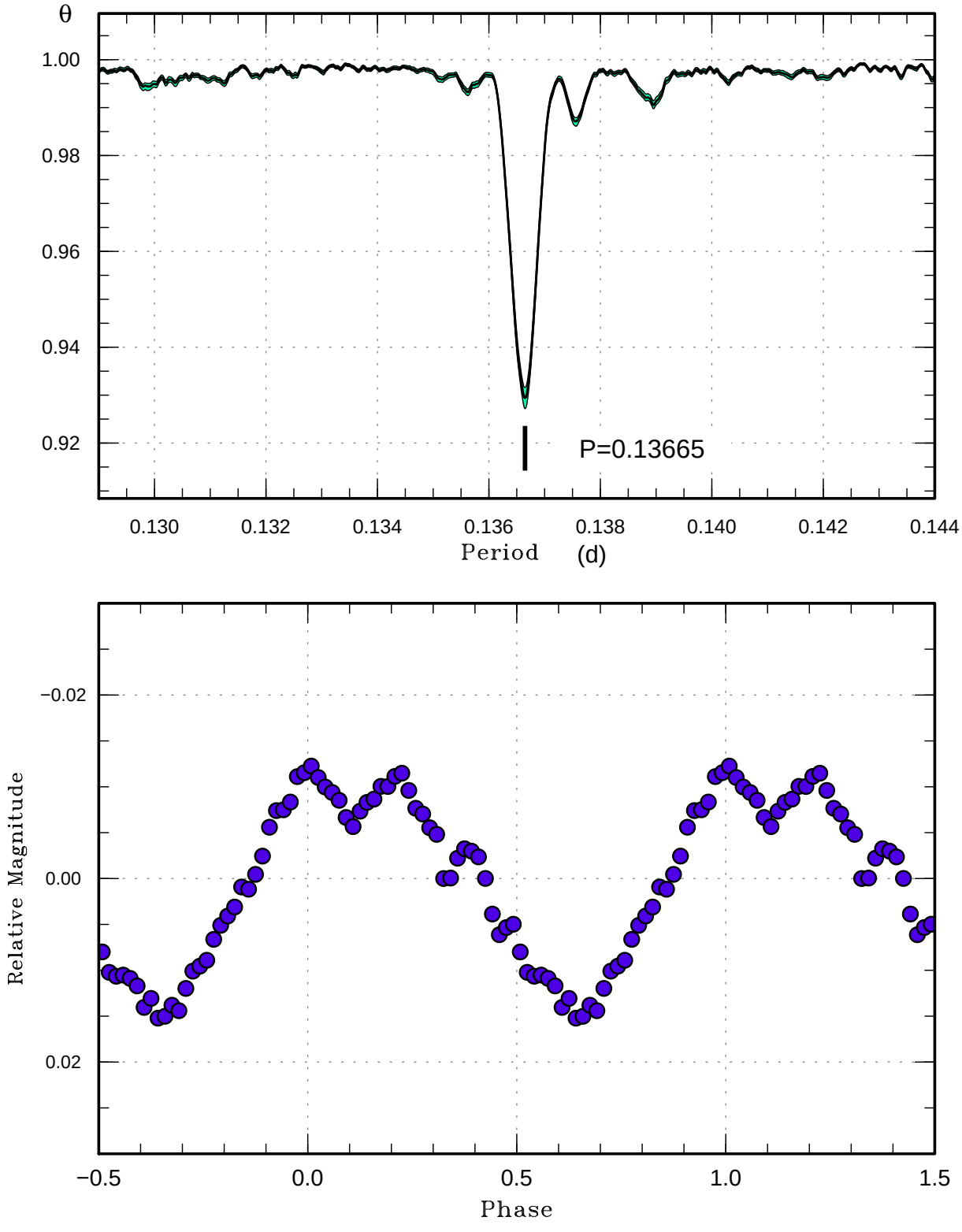

Figure 11: Period analysis of TESS data between BJD 2459390 (2021 June 25) and 2459418 (2021 July 23). These observations covered one complete outburst and one outburst during decline of the heartbeat phase. (Upper): PDM analysis. (Lower): Orbital variation.

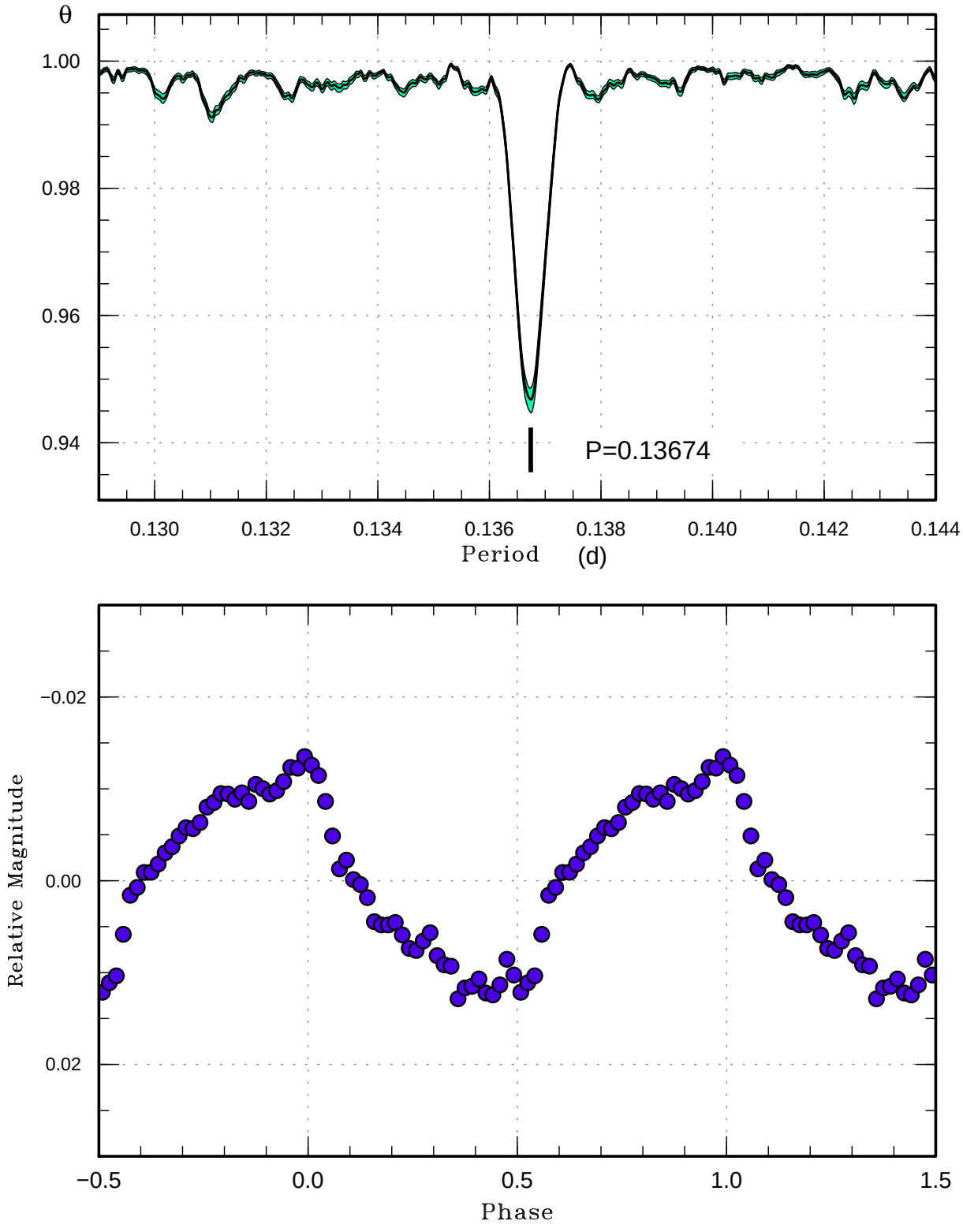

Figure 12: Period analysis of TESS data between BJD 2459579 (2021 December 23) and 2459606 (2022 January 27). These observations correspond to a slightly variable standstill phase. (Upper): PDM analysis. (Lower): Orbital variation.

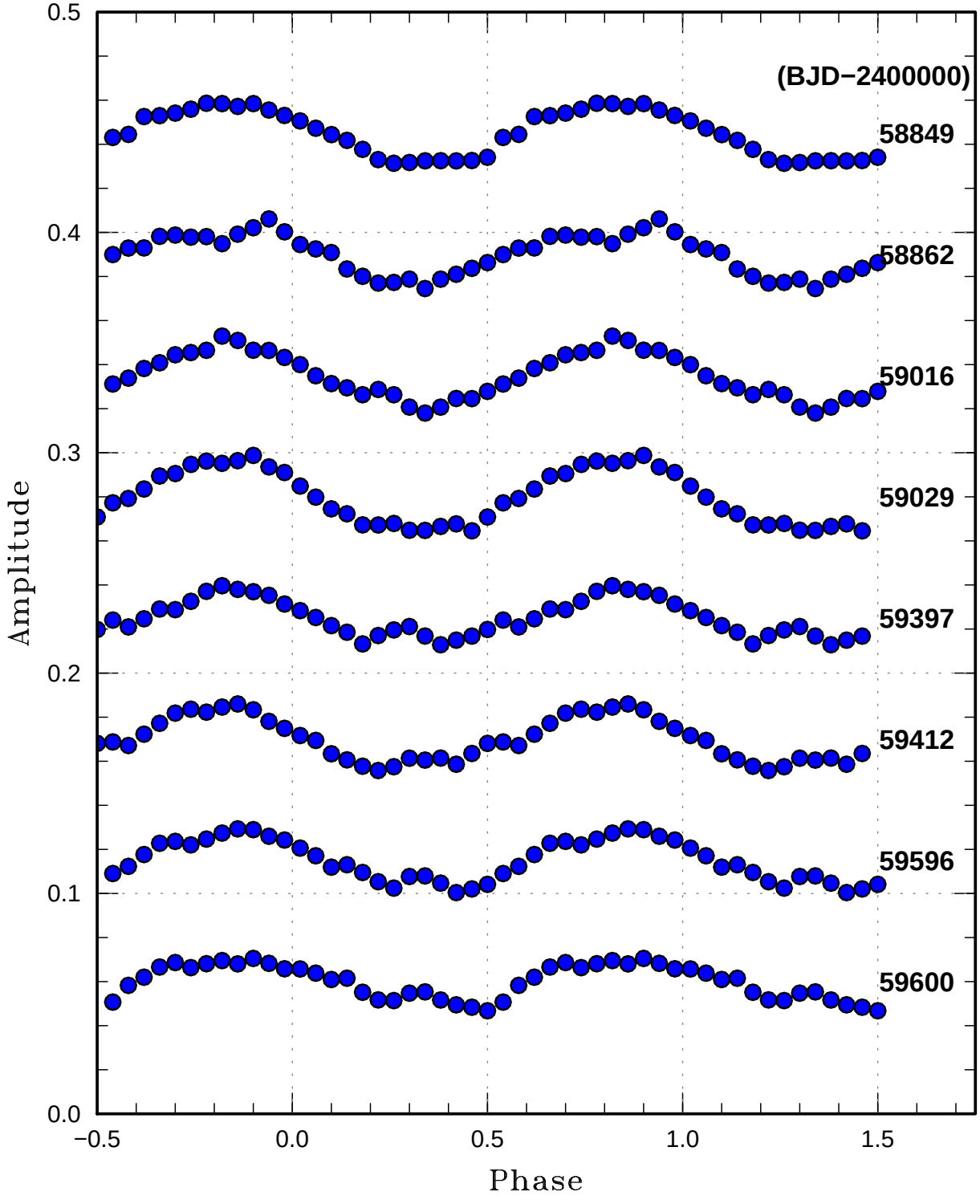

Figure 13: Variation of the orbital profile in TESS data. The data with 14-d segments centered on the dates given to the right of the averaged light curves were used. The epoch and period were from Inight et al. (2022).

Table 2: Orbital period of ASAS J071404+7004.3

Data	Interval (JD−2400000)	Period (d)	Source
Radial velocity	56597–59197	0.1366454(1)	Inight et al. (2022)
TESS (1)	58842–58868	0.136635(10)	this paper
TESS (2)	59010–59035	0.136644(7)	this paper
TESS (3)	59390–59418	0.136648(3)	this paper
TESS (4)	59579–59606	0.136741(4)	this paper
TESS combined	58842–59606	0.1366476(3)	this paper
VSNET campaign	58887–58954	0.136589(5)	this paper

(BJD 2457260–2457700) occurred when the mean magnitude was the brightest. This phenomenon challenges the classical (and widely accepted) interpretation that standstills in Z Cam stars occur when the mass-transfer rates are high (Meyer and Meyer-Hofmeister 1983).

2.6 Notes on interpretations in Inight et al. (2022)

Inight et al. (2022) suggested that there is an outer part of the disk that occasionally becomes sufficiently cool for hydrogen to recombine to explain the dwarf nova-like variations of ASAS J071404+7004.3 (this is an explanation for dwarf-nova outbursts, although Inight et al. (2022) did not adopt the dwarf-nova classification for this object) rather than periodic mass-transfer variations from the secondary as modeled by Hameury and Lasota (2014). Inight et al. (2022) stated that this outburst starts at the inner edge of this area and subsequently spreads outwards. This picture is essentially what was proposed for IW And stars in Kato (2019) (it was written as "the standstill in these objects is somehow maintained in the inner part of the disk and the thermal instability starting from the outer part of the disk terminates the standstill to complete the cycle" in the abstract). It is, however, difficult to consider a disk whose outer part becomes cool for a long time when the mass-transfer hits the outer edge of the disk. Kimura et al. (2020b) considered a tilted disk in which the majority of mass stream hits the inner disk and the outer disk is cool most of the time. Although model simulations by Kimura et al. (2020b) reproduced a limit cycle similar to IW And stars, they could not reproduce the observed disk radius variation (Kimura et al. 2020a) and the frequent occurrence of heating waves in the cool part of the disk was somewhat different from what are observed in IW And stars. The existence of the cool region in the disk of IW And stars during (quasi-)standstills has been confirmed by M. Shibata et al. in preparation and the picture by Kato (2019) and Inight et al. (2022) appear to be correct. We still need an explanation why the outer disk can remain cool in the presence of mass-transfer reaching the outer part of the disk.

Inight et al. (2022) also concluded that the emission lines in ASAS J071404+7004.3 could be reproduced by considering the wind. It would be worth noting that Tampo et al. (2022) considered the same kind of wind during the superoutburst of the WZ Sge star V455 And and reproduced singly peaked emission lines as observed, which are not expected for this high-inclination CV.

Acknowledgements

This work was supported by JSPS KAKENHI Grant Number 21K03616. The author is grateful to the ASAS-SN team for making their data available to the public. This research has made use of the AAVSO Variable Star Index and NASA's Astrophysics Data System.

List of objects in this paper

IW And, V455 And, Z Cam, V513 Cas, BO Cet, AM CVn, SS Cyg, IM Eri, V363 Lyr, HO Pup, VY Scl, WZ Sge, SU UMa, IX Vel, FY Vul, ASAS J071404+7004.3, KIC 9406652

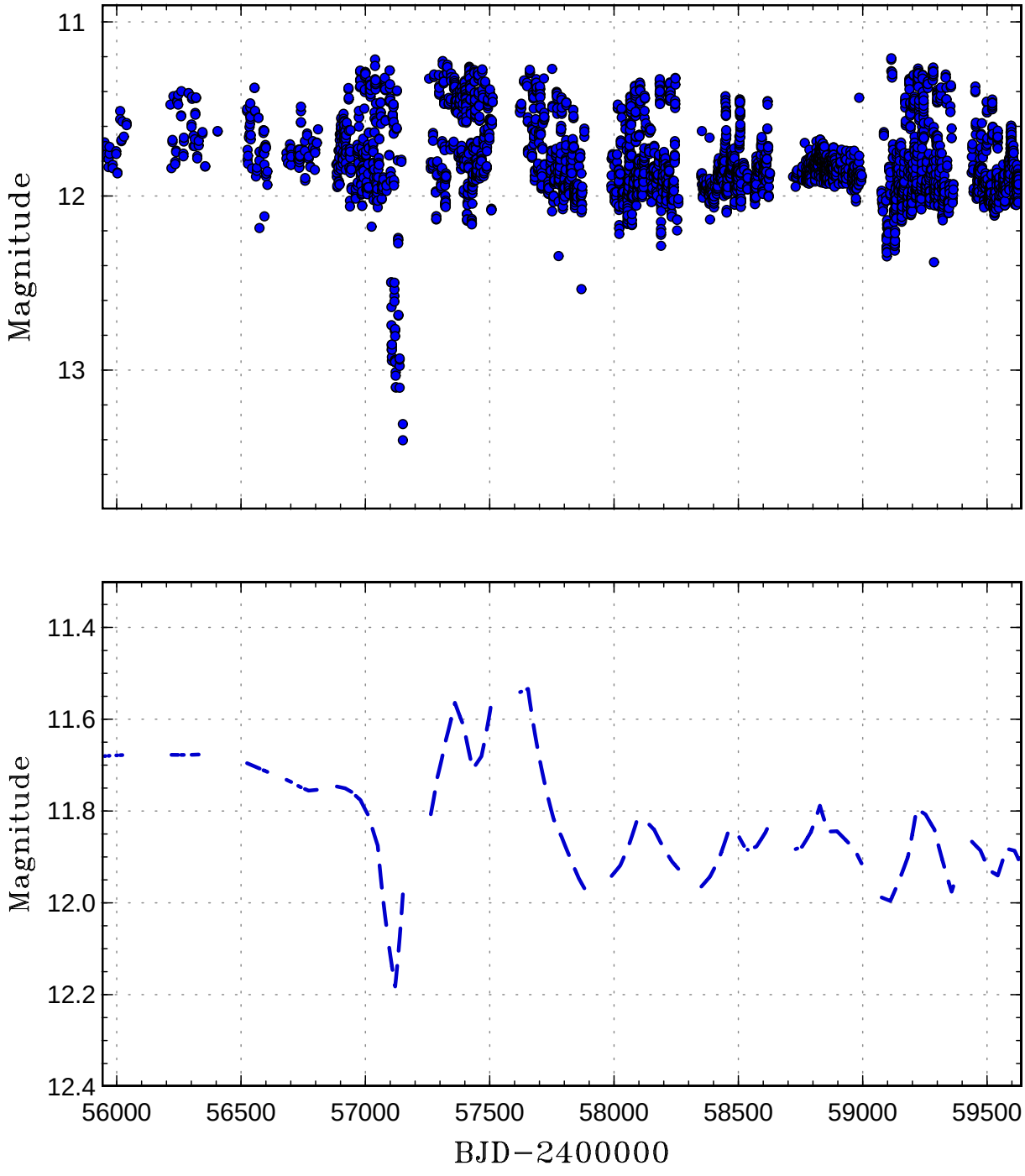

Figure 14: (Upper): ASAS-SN light curve of ASAS J071404+7004.3. (Lower): Trend determined by LOWESS. A smoothing parameter of f=0.06 was used.

References

Cleveland, W. S. (1979) Robust locally weighted regression and smoothing scatterplots. *J. Amer. Statist. Assoc.* **74**, 829

Fernie, J. D. (1989) Uncertainties in period determinations. *PASP* **101**, 225

Gies, D. R. et al. (2013) KIC 9406652: An unusual cataclysmic variable in the Kepler field of view. *ApJ* **775**, 64

Hameury, J.-M., & Lasota, J.-P. (2002) VY Sculptoris stars as magnetic CVs. *A&A* **394**, 231

Hameury, J.-M., & Lasota, J.-P. (2014) Anomalous Z Cam stars: a response to mass-transfer outbursts. *A&A* **569**, A48

Inight, K. et al. (2022) ASAS J071404+7004.3 – a close, bright nova-like cataclysmic variable with gusty winds. *MNRAS* **510**, 3605

Kato, T. (2021a) Periodic modulations during a long outburst in V363 Lyr. *VSOLJ Variable Star Bull.* **85**, (arXiv:2111.07237)

Kato, T. (2021b) Study of the low-amplitude Z Cam star IX Vel. *VSOLJ Variable Star Bull.* **87**, (arXiv:2111.15145)

Kato, T., & Hambsch, F.-J. (2021) On the nature of embedded precursors in long outbursts of SS Cyg stars as inferred from observations of the IW And star ST Cha. *VSOLJ Variable Star Bull.* **83**, (arXiv:2110.10321)

Kato, T., & Kojiguchi, N. (2021) Orbital period of the IW And-type star ST Cha. *VSOLJ Variable Star Bull.* **88**, (arXiv:2112.08552)

Kato, T. et al. (2021) BO Ceti: Dwarf nova showing both IW And and SU UMa-type features. *PASJ* **73**, 1280

Kato, T. (2019) Three Z Cam-type dwarf novae exhibiting IW And-type phenomenon. *PASJ* **71**, 20

Kato, T. et al. (2010) Survey of Period Variations of Superhumps in SU UMa-Type Dwarf Novae. II. The Second Year (2009-2010). *PASJ* **62**, 1525

Kato, T., Uemura, M., Ishioka, R., Nogami, D., Kunjaya, C., Baba, H., & Yamaoka, H. (2004) Variable Star Network: World center for transient object astronomy and variable stars. *PASJ* **56**, S1

Kato, T. et al. (2020) IW And-type state in IM Eridani. *PASJ* **72**, 11

Kimura, M., & Osaki, Y. (2021) KIC 9406652: A laboratory for tilted disks in cataclysmic variable stars. II. Modeling of the orbital light curves. *PASJ* **73**, 1225

Kimura, M., Osaki, Y., & Kato, T. (2020a) KIC 9406652: A laboratory of the tilted disk in cataclysmic variable stars. *PASJ* **72**, 94

Kimura, M., Osaki, Y., Kato, T., & Mineshige, S. (2020b) Thermal-viscous instability in tilted accretion disks: A possible application to IW Andromeda-type dwarf novae. *PASJ* **72**, 22

Kiraga, M., & Stępień, K. (2013) ASAS photometry of ROSAT Sources. II. New variables from the ASAS North Survey. *Acta Astron.* **63**, 53

Kochanek, C. S. et al. (2017) The All-Sky Automated Survey for Supernovae (ASAS-SN) light curve server v1.0. *PASP* **129**, 104502

Kotko, I., Lasota, J.-P., Dubus, G., & Hameury, J.-M. (2012) Models of AM Canum Venaticorum star outbursts. *A&A* **544**, A13

Leach, R., Hessman, F. V., King, A. R., Stehle, R., & Mattei, J. (1999) The light curves of VY Scl stars. *MNRAS* **305**, 225

Lee, C.-D. et al. (2021) HO Puppis: Not a Be star, but a newly confirmed IW And-type star. *ApJ* **911**, 51

Meyer, F., & Meyer-Hofmeister, E. (1983) A model for the standstill of the Z Camelopardalis variables. *A&A* **121**, 29

Pojmański, G. (2002) The All Sky Automated Survey. Catalog of variable stars. I. 0^h–6^h quarter of the southern hemisphere. *Acta Astron.* **52**, 397

Shappee, B. J. et al. (2014) The man behind the curtain: X-rays drive the UV through NIR variability in the 2013 AGN outburst in NGC 2617. *ApJ* **788**, 48

Stellingwerf, R. F. (1978) Period determination using phase dispersion minimization. *ApJ* **224**, 953

Tampo, Y. et al. (2022) Spectroscopic observations of V455 Andromedae superoutburst in 2007: the most exotic spectral features in dwarf nova outbursts. *PASJ* **in press (arXiv/2201.09094)**

Tsugawa, M., & Osaki, Y. (1997) Disk instability model for the AM Canum Venaticorum stars. *PASJ* **49**, 75

Voges, W. et al. (1999) The ROSAT all-sky survey bright source catalogue. *A&A* **349**, 389

Warner, B. (1995) The AM Canum Venaticorum stars. *Ap&SS* **225**, 249

Watson, C. L., Henden, A. A., & Price, A. (2006) The International Variable Star Index (VSX). *Society for Astronom. Sciences Ann. Symp.* **25**, 47

VSOLJ
c/o Keiichi Saijo National Science Museum, Ueno-Park, Tokyo Japan

Editor Seiichiro Kiyota
e-mail: skiyotax@gmail.com